ROZPRAWY INŻYNIERSKIE • ENGINEERING TRANSACTIONS • 37, 2, 375–397, 1989
Polska Akademia Nauk • Instytut Podstawowych Problemów Techniki

INTERACTIVE BUCKLING OF THIN-WALLED BEAMS WITH OPEN AND CLOSED CROSS-SECTIONS

Z. KOŁAKOWSKI (ŁÓDŹ)

Influence of the interaction of nearly simultaneous buckling modes on the postbuckling behaviour of thin-walled beams with imperfections is studied. The investigation is concerned with thin-walled closed and open cross-section elastic beams under an axial compression and a constant bending moment. The beams are assumed to be simply supported at the ends. The asymptotic expansion established by BYSKOV and HUTCHINSON [1] is employed in the numerical calculations in the form of the transition matrix method. The paper's aim is to achieve the improved study of the equilibrium path in the initial postbuckling behaviour of imperfect structures in which the effect of the interaction of a few buckling modes would be included. The calculations are carried out for several types of beams.

1. NOTATION

a_{ijJ} postbuckling coefficients (see BYSKOV and HUTCHINSON [1]),
b_i width of the i-th wall of the beam,
D_i flexural rigidity of the i-th wall,
E Young's modulus,
h_i thickness of the i-th wall of the beam,
l length of the beam,
m number of axial half-waves of mode n,
M_{ix}, M_{iy}, M_{ixy} bending moment resultants for the i-th wall,
n number of mode,
N_{ix}, N_{iy}, N_{ixy} in-plane stress resultants for the i-th wall,
Q_{iy} Eqn. (3.5),
u_i, v_i, w_i displacement of middle surface,
$\overset{0}{u}_i, \overset{0}{v}_i, \overset{0}{w}_i$ prebuckling displacement fields,
$\overset{n}{u}_i, \overset{n}{v}_i, \overset{n}{w}_i$, buckling displacement fields,
Λ load factor,
η, ϑ global coordinate system of the beam,
λ scalar load parameter,
λ_n value of λ at bifurcation mode number n,
λ_s maximum value of λ for imperfect beam,
ξ_n amplitude of buckling mode number n,
$\bar{\xi}_n$ imperfection amplitude corresponding to ξ_n,
$\sigma_m^* = \min(\sigma_1^* .. \sigma_n^*)$,
$\sigma_n^* = \sigma_n 10^3/E$ dimensionless stress of mode number n,
σ_s^* limit dimensionless stress for imperfect beam.

2. INTRODUCTION

Thin-walled elements are widely used as structural components in many types of metal structures in which the interaction buckling of elastic beams may result in an imperfection-sensitive structure and is the principal cause of collapse of thin-walled structures. Such problems often arise in connection with optimal structural design.

KOITER and van der NUET [2] have proposed a technique in which the interaction of an overall mode with two local modes having the same wavelength have been considered. The fundamental mode is henceforth called "primary" and the notrivial higher mode (having the same wavelength as the "primary") corresponding to the mode triggered by overall longwave mode is called "secondary".

SRIDHARAN and ALI [3] have presented an analysis of 3-mode interaction using a finite strip method for thin-walled columns having doubly symmetric cross-sections and in which the secondary order solution has been used.

MØLLMANN and GOLTERMANN [4,5] have studied the postbuckling behaviour and the imperfection-sensitivity, the buckling modes and the 2-nd order displacement fields being determined by the finite strip method. The method has been based on Koiter's asymptotic theory of stability.

PIGNATARO and LUONGO [6] have analysed the interaction of buckling modes in thin-walled open columns on the ground of the general theory of elastic stability and using third-order term of the energy expansion of the finite strip method.

Paper [7] has been devoted to an analysis of the interactive buckling of the trapezoidal column in the initial postbuckling behaviour. However, a 3-mode approach analysis is introduced in the four latest papers [4–7].

BYSKOV [8] has proved that very few of local modes need to be taken into account for the particular structure – i.e. van der Neut's column possesing an "infinitely many" nearly simultaneous local modes but having only the different wavelength.

Some works concerning the interactions between the only two independent buckling modes of thin-walled structures have been done by BENITO and SRIDHARAN [9], HUI [10], BYSKOV [11], KOŁAKOWSKI [12].

In the present paper the initial postbuckling behaviour of thin-walled structures in the elastic range being under an nonuniform compression is examined on the basis of Byskov and Hutchinson's method with the co-operation between all the walls of the structures being taken into account. The study of the interaction modes is based on the determination of the transition matrix. The background of this method has been discussed in the papers [13–15]. An attractive feature of this method is that it is capable of describing the complete range of behaviour of the thin-walled structures from

global to local stability. In the solution obtained, the effects of interaction of certain modes having the same wavelength, the shear lag phenomenon and also the effect of cross-sectional distorsions are included.

3. Structural problem

The long thin-walled prismatic beams of a length l and composed of plane, rectangular plate segments interconnected along longitudinal edges, simply supported at both ends are considered for which $b_i/l \ll 1$.

Cross-section of this structure consists of a few plates and assumed local Cartesian coordinate systems are presented in Fig. 1.

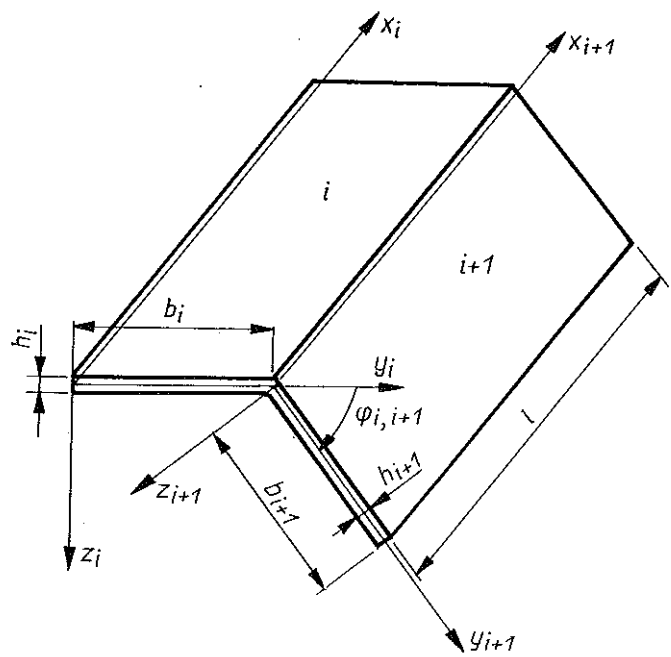

FIG. 1. Prismatic plate structure and the local coordinate system.

The membrane strains of the i-th wall are as follows:

$$\begin{aligned} \varepsilon_{ix} &= u_{i,x} + 0.5(w_{i,x}^2 + v_{i,x}^2), \\ \varepsilon_{iy} &= v_{i,y} + 0.5(w_{i,y}^2 + u_{i,y}^2), \\ \gamma_{ixy} &= u_{i,y} + v_{i,x} + w_{i,x} w_{i,y}. \end{aligned} \tag{3.1}$$

The bending strains are given by

$$\varkappa_{ix} = -w_{i,x}, \quad \varkappa_{iy} = -w_{i,y}, \quad \varkappa_{ixy} = -w_{i,xy}. \tag{3.2}$$

The differential equilibrium equations resulting from the virtual work expression for single wall can be written as:

$$\begin{aligned} &-N_{ix,x} - N_{ixy,y} - (N_{iy} u_{i,y})_{,y} = 0, \\ &-N_{iy,y} - N_{ixy,x} - (N_{ix} v_{i,x})_{,x} = 0, \\ &D_i \nabla\nabla w_i - (N_{ix} w_{i,x})_{,x} - (N_{iy} w_{i,y})_{,y} - (N_{ixy} w_{i,x})_{,y} - (N_{ixy} w_{i,y})_{,x} = 0. \end{aligned} \tag{3.3}$$

The geometrical and statical continuity conditions at the junctions of plates may be written in the form:

$$\begin{aligned} &u_{i+1}|^0 = u_i|^+, \\ &w_{i+1}|^0 = w_i|^+ \cos\phi - v_i|^+ \sin\phi, \\ &v_{i+1}|^0 = w_i|^+ \sin\phi + v_i|^+ \cos\phi, \\ &w_{i+1,y}|^0 = w_{i,y}|^+, \\ &D_{i+1}(w_{i+1,yy} + \nu w_{i+1,xx})|^0 - D_i(w_{i,yy} + \nu w_{i,xx})|^+ = 0, \\ &N_{i+1y}|^0 - N_{iy}|^+ \cos\phi - Q_{iy}|^+ \sin\phi = 0, \\ &Q_{i+1y}|^0 + N_{iy}|^+ \sin\phi - Q_{iy}|^+ \cos\phi = 0, \\ &N_{i+1xy}|^0 - N_{ixy}|^+ = 0, \end{aligned} \tag{3.4}$$

where

$$Q_{iy} = N_{iy} w_{i,y} + N_{ixy} w_{i,x} - D_i(w_{i,yyy} + (2-\nu) w_{i,xxy}) \qquad \phi \equiv \phi_{i,i+1}. \tag{3.5}$$

The prebuckling solution consists of homogeneous fields which is assumed as:

$$\overset{0}{u}_i = -x_i \Delta, \quad \overset{0}{v}_i = \nu y_i \Delta, \quad \overset{0}{w}_i = 0, \tag{3.6}$$

where Δ is a linear function of y according to the actual loading. This loading is specified as the product of a unit loading system and a scalar load factor Δ. The boundary conditions permit the first order solution to be written:

$$\overset{n}{u}_i = \overset{n}{U}_i(y) \cos\frac{m\pi x_i}{l}, \quad \overset{n}{v}_i = \overset{n}{V}_i(y) \sin\frac{m\pi x_i}{l}, \quad \overset{n}{w}_i = \overset{n}{W}_i(y) \sin\frac{m\pi x_i}{l}, \tag{3.7}$$

where $\overset{n}{U}_i(y)$, $\overset{n}{V}_i(y)$, $\overset{n}{W}_i(y)$ (with m-th harmonic) are initially unknown functions which will be determined using the transition matrix method [13–15]. The restraint conditions on the unloaded longitudinal edges of the adjacent plates are determined by applying the variational principle. The system of the differential equilibrium equations (3.3) is solved by a modified reduction

method in which the state vector of the final edge is derived from the state vector of the initial edge by numerical integration of the differential equations in the y-direction using the Runge–Kutte formulae.

The global buckling mode occurs at $m = 1$ and the local modes occur at $m \neq 1$. All the modes are normalized so that the maximum normal displacement is equal to unity.

The formulae for the postbuckling coefficients a_{ijJ} involve only the buckling modes. In the points where the scalar load parameters λ_s reach the maximum value for the imperfect structure (bifurcation or limit points), the Jacobian of system of non-linear equations [1]:

$$\xi_J(-\lambda/\lambda_J)+\xi_i\xi_j a_{ijJ}+\ldots:=\lambda/\lambda_J\,\overline{\xi}_J \quad \text{at} \quad J=1,..n \tag{3.8}$$

is equal to zero. The postbuckling coefficients a_{ijJ} are equal to zero when the sum of te wave numbers associated with the three modes $(m_i+m_j+m_k)$ is an even number.

4. Results

A computer program has been elaborated and tested for cases which have been known from the literature [4, 5, 7, 9, 12, 14, 15]. In all tested cases a very good agreement has been found with results known from the literature; the only exception has been observed in [12] (item 3, Table 1, p. 338). In this case the nonlinear coefficients d_2 and d_3 should be zero. The above numerical error has been caused by the improperly conditioned input data vector.

The detailed numerical calculations for some beams, geometry of which is given in references [4, 5, 7, 9, 12, 14], have been performed.

4.1. Closed column

The solid line in Fig. 3 represents the results obtained in the paper [5] (for 3-mode approach of 1-st order fields) for a compressive thin-walled column of square cross-section (Fig. 2)

$$b_1/b_2 = 1.0, \quad b_3/b_2 = 1.0, \quad h_1/h_2 = 1.0, \quad h_3/h_2 = 1.0,$$
$$l/b_2 = 24.0, \quad b_2/h_2 = 35.0, \quad \nu = 0.3$$

while crosses show the results obtained in the present paper. For a square column, the geometrical dimensions of which are the following [7, 12]:

$$b_1/b_2 = 1.0, \quad b_3/b_2 = 1.0, \quad h_1/h_2 = 1.0, \quad h_3/h_2 = 1.0,$$
$$l/b_2 = 67.39, \quad b_2/h_2 = 100.0, \quad \nu = 0.3.$$

Fig. 4 presents a relation of the dimensionless stress σ_n^* instead of load

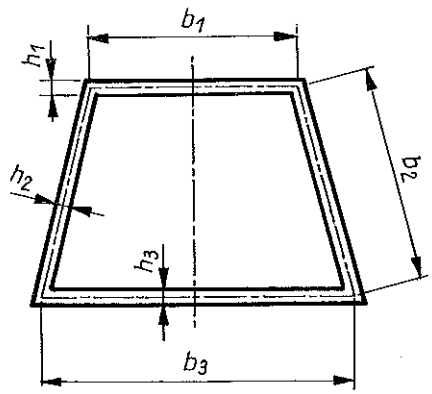

FIG. 2. Closed-column geometry.

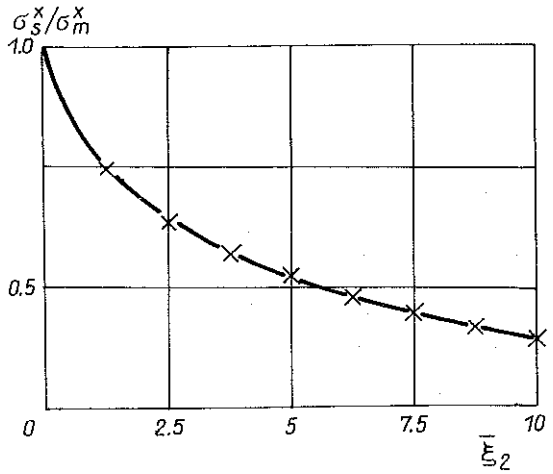

FIG. 3. Load-carrying capacity σ_s^* versus local imperfection $\bar{\xi}_2$.

parameter λ_n (where index n takes the value 2 in the primary local buckling mode and 3 in the secondary local mode) in terms of number of half-waves m, and in Fig. 5 the ratio of the dimensionless limit stress σ_s^* to the lowest dimensionless stress σ_m^* as the function of m for imperfections $\bar{\xi}_1 = |1.0|$, $\bar{\xi}_2 = |0.2|$, $\bar{\xi}_3 = 0.0$. In these figures the maximum of load carrying capacity (σ_s^*) is marked by a crosslet. In each case the signs of the imperfections $\bar{\xi}_1$ and $\bar{\xi}_2$ have been chosen in the most infavourable fashion, i.e. so that σ_s^* would assume its minimum value (see [7, 12, 16] for a more detailed discussion). It can be easily noticed that the maximum value of σ_s^* (for steady values of the imperfections) and the minimum values of σ_2^* and σ_3^* (Fig. 4) are, in general, achieved at different values of m. The complex nature of the dependence of

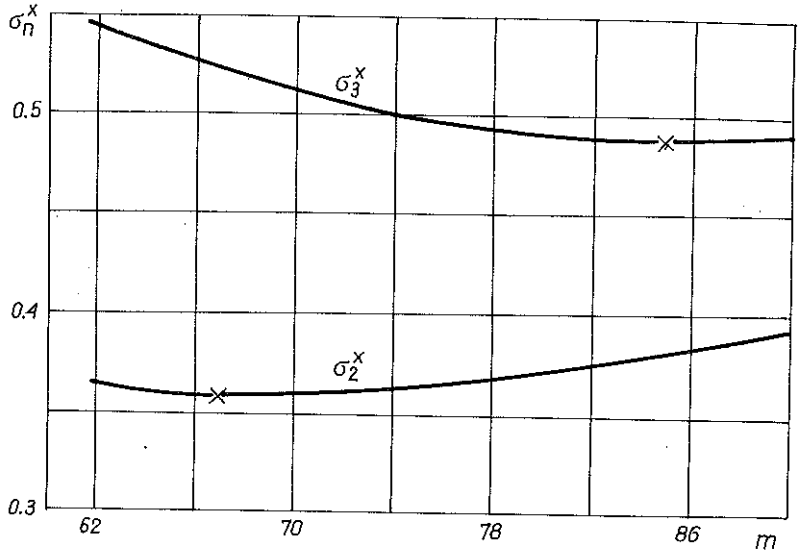

FIG. 4. Dimensionless stresses σ_n^* carried by the numbers of half-waves m for square box-column.

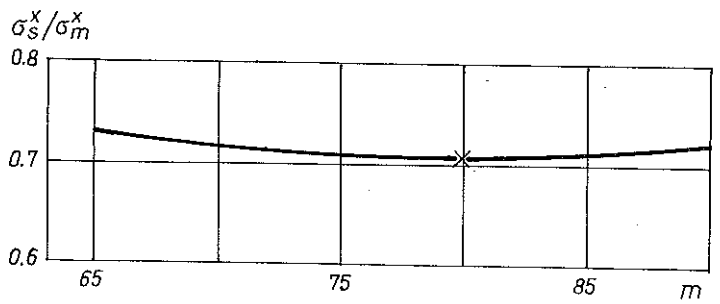

FIG. 5. Relationship between σ_s^* and number of half-waves m for square box-column.

σ_s^* against number of half-waves m results in the most dangerous local modes in linear and nonlinear analysis possibly being different.

The global buckling modes are illustrated in Fig. 6 and a few first local buckling modes at $m = 67$ in Fig. 7.

Table 1 contains values of nondimensional stresses σ_n^*, in brackets, numbers of half-waves m and the ratios of the dimensionless limit stress σ_s^* to the dimensionless stress σ_m^* for the imperfections $\bar{\xi}_1 = |1.0|$, $\bar{\xi}_2 = |0.2|$, $\bar{\xi}_j = 0.0$ (at $j = 3, .. n$) and for some possible combinations of buckling modes, presented in Figs. 6, 7. The following code has been used in Tabl. 1 in order to identify support conditions at element edges: 1 — antisymmetry on the axis of the symmetry of the cross-section; 2 — symmetry on the axis of the symmetry; 3 — a completely free edge ($M_y = Q_y = N_y = N_{xy} = 0$), respectively, for the i-th buckling mode. The postbuckling coefficients a_{iij} generally vanish, i.e. $a_{iik} = 0$

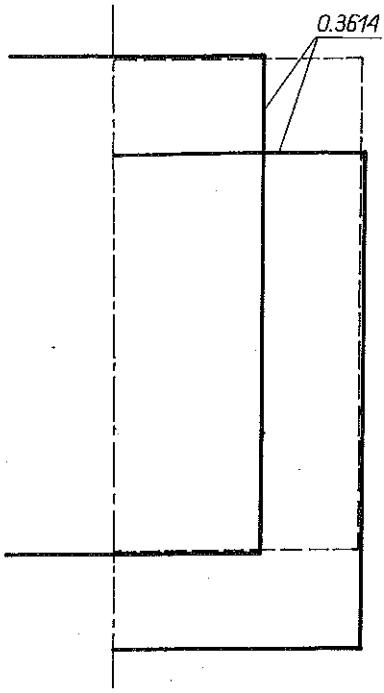

FIG. 6. Two first global modes for square box-column.

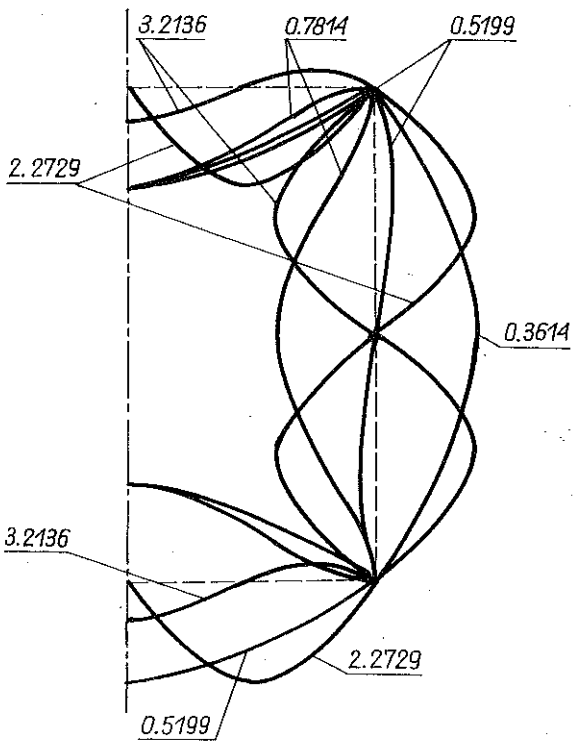

FIG. 7.Several local modes for square box-column.

Table 1. Load-carrying capacity for the square column of following cross-section dimensions $b_1/b_2 = b_3/b_2 = 1.0$, $h_1/h_2 = h_3/h_2 = 1.0$, $l/b_2 = 67.39$, $b_2/h_2 = 100.0$, **at imperfections** $\bar{\xi}_1 = |1.0|$, $\bar{\xi}_2 = |0.2|$, $\bar{\xi}_i = 0.0$ $(i = 3, \ldots, n)$.

Interaction of n-mode	σ_1^*	σ_2^*	σ_3^*	σ_4^*	σ_5^*	σ_s^*/σ_m^*
1 5–22211	0.3614(1)	0.3614(67)	0.5199(67)	0.3614(1)	0.5199(67)	0.7213
2 5–22222	03614(1)	0.3614(67)	0.5199(67)	0.3619(65)	0.3616(69)	0.7191
3 5–22222	0.3614(1)	0.3614(67)	0.5199(67)	0.5287(65)	0.5124(69)	0.7077
4 5–22222	0.3614(1)	0.3614(67)	0.5199(67)	0.3631(63)	0.3624(71)	0.7212
5 5–22222	0.3614(1)	0.3614(67)	0.5199(67)	0.5389(63)	0.5062(71)	0.7207
6 5–22222	0.3614(1)	0.3614(67)	0.5199(67)	0.7814(67)	3.2136(67)	0.7196
7 4–2222	0.3614(1)	0.3614(67)	0.5287(65)	0.5124(69)		0.8096
8 4–2222	0.3614(1)	0.3614(67)	0.5199(67)	0.4904(80)		0.7213
9 3–222	0.3614(1)	0.3614(67)	0.5199(67)			0.7213
10 3–121	0.3614(1)	0.3614(67)	0.5199(67)			0.7213
11 3–121	0.3614(1)	0.3614(67)	3.2136(67)			0.9528
12 3–222	0.3614(1)	0.3722(80)	0.4904(80)			0.7052
13 2–22	0.3614(1)	0.3614(67)				$a_{ijJ} = 0$

at $i, j, k = 1, .., n$ except that $a_{ijk} \neq 0$ at $i \neq j \neq k$ for beams having doubly symmetric sections. The results obtained allow to conclude that in the case of the interaction between Euler buckling mode and the primary local buckling mode and the corresponding secondary having the same shape as the global one is of great importance. This effect is contained in the term $\sigma_1 \cdot l_{11}(u_i, u_j)$ (where $i, j = 2, 3$) in coefficients a_{ijJ} of the equations (3.8) which are the sums of integrals of different signs and they depend on the ratios of amplitudes of displacements of particular walls. The dominant coefficients are those for which number of local half-waves m_i is of the order m_j. If $|m_i - m_j| \gg 0$ these coefficients in particular can be neglected. The lowest value of stress σ_s^* has been found in the 3-mode approach, taking into account the influence of the value of imperfection on the number of half-waves m (case 12). A similar result has been obtained when an interaction of five buckling modes has been considered (case 3): the global mode, the first least local mode ($m = 67$), the second local mode corresponding to the latter, and two local modes corresponding to the mode triggered by the global one and having the number of half-waves of two last modes $m \pm 2$ (according to what is suggested in [8]).

The next four diagrams (Figs. 8–11) and Table 2 show respective dependences for a column of trapezoidal cross-section (Fig. 2):

$$b_1/b_2 = 0.5237, \quad b_3/b_2 = 1.0474, \quad h_1/h_2 = 0.4651,$$
$$h_3/h_2 = 1.5814, \quad l/b_2 = 46.095, \quad b_2/h_2 = 88.8, \quad \nu = 0.3.$$

The conclusions that can be drawn from the calculations of the cross-section

Table 2. Load-carrying capacity for the trapezoidal column of following cross-section dimensions
$b_1/b_2 = 0.5237$, $b_3/b_2 = 1.0474$, $h_1/h_2 = 0.4651$
$h_3/h_2 = 1.5814$, $l/b_2 = 46.095$, $b_2/h_2 = 88.8$
at imperfections $\bar{\xi}_1 = |1.0|$, $\bar{\xi}_2 = |0.2|$, $\bar{\xi}_i = 0.0$ $(i = 3, \ldots, n)$.

Interaction of n-mode	σ_1^*	σ_2^*	σ_3^*	σ_4^*	σ_5^*	σ_s^*/σ_m^*
1 5–22211	0.5677(1)	0.5659(53)	1.1992(53)	0.5657(1)	0.6148(53)	0.6820
2 5–22222	0.5677(1)	0.5659(53)	1.1992(53)	0.5671(51)	0.5662(55)	0.6699
3 5–22222	0.5677(1)	0.5659(53)	1.1992(53)	1.2023(51)	1.1884(55)	0.6861
4 5–22222	0.5677(1)	0.5659(53)	1.1992(53)	0.5699(49)	0.5678(57)	0.6866
5 5–22222	0.5677(1)	0.5659(53)	1.1992(53)	1.2102(49)	1.1722(57)	0.6875
6 5–22222	0.5677(1)	0.5659(53)	1.1992(53)	1.4144(53)	3.4290(53)	0.6847
7 4–2222	0.5677(1)	0.5659(53)	1.2023(51)	1.1884(55)		0.6938
8 4–2222	0.5677(1)	0.5659(53)	1.1992(53)	0.5982(69)		0.6876
9 3–222	0.5677(1)	0.5659(53)	1.1992(53)			0.6876
10 3–121	0.5657(1)	0.5659(53)	0.6148(53)			0.6901
11 3–121	0.5657(1)	0.5659(53)	3.0546(53)			0.9567
12 3–222	0.5677(1)	0.5982(69)	0.9578(69)			0.6543
13 2–22	0.5677(1)	0.5659(53)				0.6957

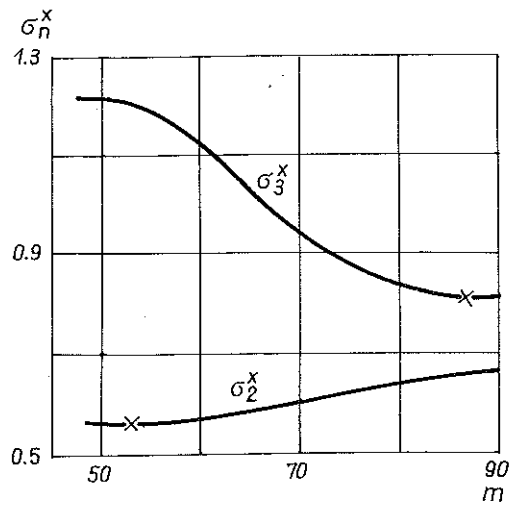

FIG. 8. Dimensionless stresses σ_n^* carried by the number of half-waves m for trapezoidal column.

with a single symmetry axis (Figs. 8, 9; Tabl. 2) are analogous to those in the case of the two-fold axis of symmetry (Figs. 4. 5: Tabl. 1).

In the energy expression the coefficients of the cubic terms $\xi_1 \xi_2^2$, $\xi_1 \xi_3^2$ and $\xi_1 \xi_2 \xi_3$ are the key term governing the interaction. In the case disregarding the interaction between overall mode and the primary local mode and the secondary local mode, the coefficient of the $\xi_1 \xi_2 \xi_3$ term in the energy

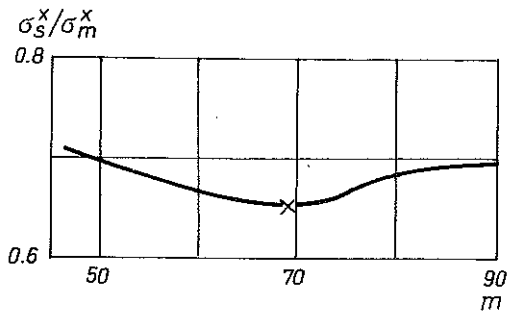

FIG. 9. Relationsip between σ_s^* and number of half-waves m for trapeziodal column.

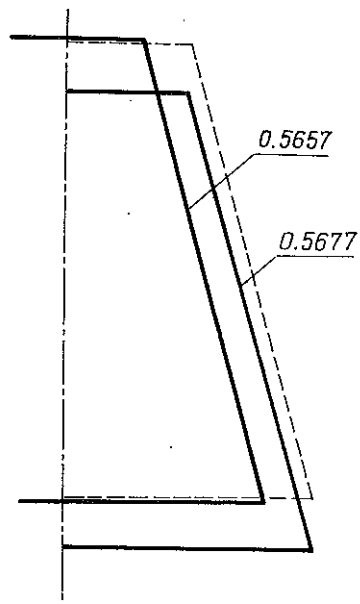

FIG. 10. Two first global modes for trapezoidal column.

expression vanishes (see [3, 4, 5, 7]). The analysis of column [3] with doubly symmetric cross-sections shows that the cofficients of the $\xi_1 \xi_2^2$ and $\xi_1 \xi_3^2$ terms (Tabl. 1 — case 13) vanish. The exception is connected with the fact that in the calculation of the section with the single symmetry axis only the interaction of the overall buckling mode with the local mode can be taken into account (Tabl. 2 — case 13). In the considered case the influence of the second local buckling mode cannot be neglected (Tabl. 2 — compare cases 12 and 13) because the error is 6.3 per cent.

MANEVICH [16] has determined a post-bifurcational equilibrium path of an infinitely wide plate with thin-walled stiffeners. Manevich presents a theory which, in terms of the first nonlinear approximation, allows to determine the

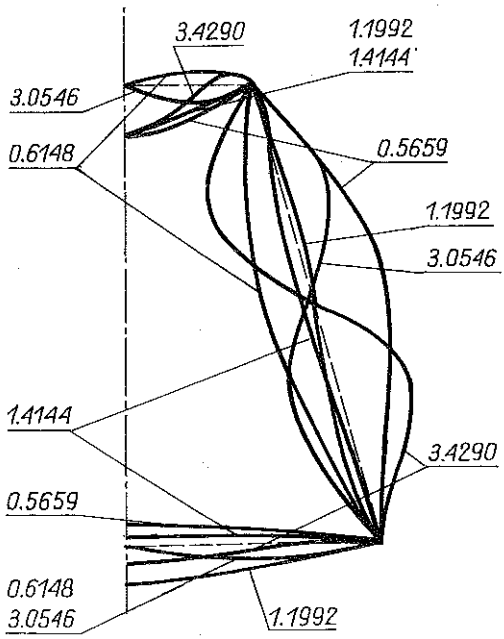

FIG. 11. Several local modes for trapezoidal column.

relation between the system with several modes and that of one local buckling mode. The theory is valid in the case of symmetrical characteristic of the global ($a_{111} = 0$) and several different local buckling modes with different numbers of halfwaves m. If $n-1$ local modes are considered, the only interaction which can be taken into account is that of two modes: the global and the most dangerous local one, having assumed an equivalent value of local imperfection. A σ_s^* to σ_m^* ratio has been determined for the column of the trapezoidal cross-section, analyzed above; the value of the global imperfection $\bar{\xi}_1 = |1.0|$ and of the equivalent local imperfection $\bar{\xi}_2^*$ corresponding to a local imperfection $\bar{\xi}_2 = |0.2|$ ($\bar{\xi}_3 = 0.0$); an interaction of the two local buckling modes has been considered. The resulting value of σ_s^*/σ_m^* is 0.6552. This is close to the value corresponding to case 12 in Table 2.

4.2. Open beams

The interactive buckling of thin-walled open beams has been investigated in cold formed steel structures.

Figures 12 show the cross-sections of the considered beams. Let us consider the channel-section beam analysed in [9] dimensions of which are (Fig. 12.a):

$$b_1/b_2 = 0.5, \quad b_3/b_2 = 0.5, \quad h_1/h_2 = 1, \quad h_3/h_2 = 1,$$
$$b_2/h_2 = 50, \quad l/b_2 = 13$$

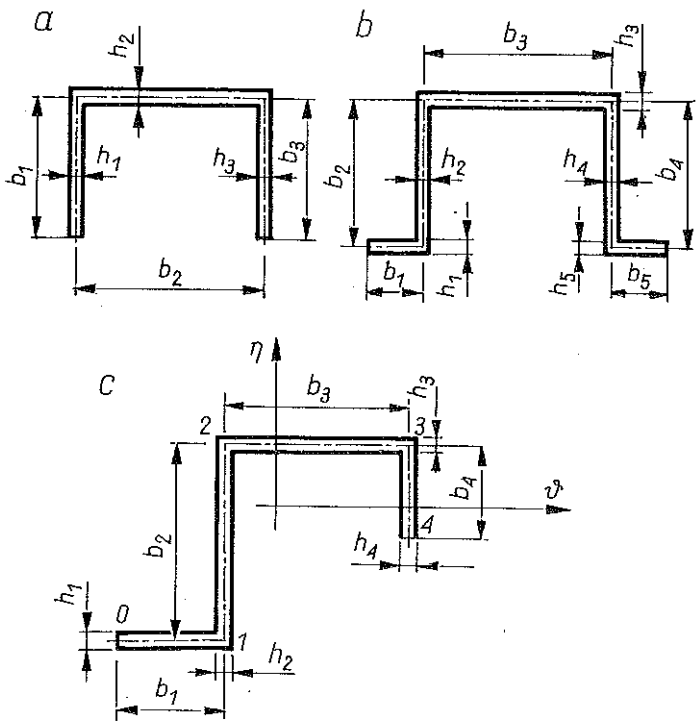

FIG. 12. Types of open cross-sections considered.

The ratio of the flexural-torsional (primary global) stress to the primary local stress is found here as equal to 0.99 and the ratio of purely flexural (secondary global) stress to the primary local stress is determined as equal to 1.42 (in the paper [9] these rations are 1.04 and 1.44, respectively).

Table 3, similarly to Tables 1 and 2, comprises the values of nondimensional stress σ_n^* and the ratio σ_s^*/σ_m^* for imperfections $\bar{\xi}_1 = |1.0|$, $\bar{\xi}_2 = |0.2|$, $\bar{\xi}_i = 0.0$ (at $i = 3, \ldots n$) and for some possible combinations of buckling modes; indexation remains the same as previously. The calculations carried out readily show that the most dangerous case is an interaction of the second global mode with local modes (compare cases 8 and 16). The local mode imperfections always promote an interaction between the local mode(s) and the global mode (compare cases 1,2 and 3,4: 5, 6, 7 and 8, 16). Moreover, one can see that the interaction of two global modes of buckling is very weak or even does not occur at all (compare cases 5, 6, 8 and 16). It can be noticed that the Euler buckling can interact with an even number of local modes symmetric or antisymmetric but the flexural-torsional mode only with pairs of symmetric and antisymmetric modes (see [6] for more detailed analysis). In these cases $a_{ijJ} \neq 0$ and in the others $a_{ijJ} = 0$ (case 9). In some cases an improper selection

Table 3. Load-carrying capacity for the open column of following cross-section dimensions $b_1/b_2 = 0.5$, $b_3/b_2 = 0.5$, $h_1/h_2 = 1.0$, $h_3/h_2 = 1.0$, $b_2/h_2 = 50.0$, $l/b_2 = 13.0$ **at imperfections** $\bar{\xi}_1 = |1.0|$, $\bar{\xi}_2 = |0.2|$, $\bar{\xi}_i = 0.0$ $(i = 3, \ldots, n)$.

Interaction of n-mode	σ_1^*	σ_2^*	σ_3^*	σ_4^*	σ_5^*	σ_s^*/σ_m^*
1 5–33333	1.0434(1)	1.4908(1)	1.0513(10)	1.4399(10)	3.3079(10)	0.7932
2 5–33333	1.0434(1)	1.4908(1)	1.0513(10)	1.4399(10)	16.779(10)	0.7951
3 5–33333	1.0434(1)	1.0513(10)	1.4399(10)	1.0818(8)	1.0857(12)	0.7093
4 5–33333	1.0434(1)	1.0513(10)	1.4399(10)	1.6510(8)	1.3734(12)	0.7015
5 4–3333	1.0434(1)	1.4908(1)	1.0513(10)	3.3079(10)		0.8409
6 4–3333	1.0434(1)	1.4908(1)	1.0513(10)	1.4399(10)		0.7961
7 3–333	1.0434(1)	1.4908(1)	1.0513(10)			0.8416
8 3–333	1.0434(1)	1.0513(10)	1.4399(10)			0.7153
9 3–333	1.0434(1)	1.0513(10)	3.3079(10)			$a_{ijJ} = 0$
10 3–333	1.0434(1)	1.0513(10)	16.779(10)			0.8917
11 5–33333	1.4908(1)	1.0513(10)	1.4399(10)	1.6510(8)	1.3734(12)	0.6442
12 5–33333	1.4908(1)	1.0513(10)	1.4399(10)	1.0818(8)	1.0857(12)	0.6144
13 5–33333	1.4908(1)	1.0513(10)	1.4399(10)	4.4305(8)	2.7337(12)	0.6411
14 5–33333	1.4908(1)	1.0513(10)	3.3079(10)	4.4305(8)	2.7337(12)	0.6255
15 3–333	1.4908(1)	1.0513(10)	1.4399(10)			0.6450
16 3–333	1.4908(1)	1.0513(10)	3.3079(10)			0.6287
17 3–333	1.4908(1)	1.0513(10)	16.779(10)			0.6450
18 2–33	1.4908(1)	1.0513(10)				0.6450
19 2–33	1.0434(1)	1.0513(10)				$a_{ijJ} = 0$

of mode, even if a few of them are considered, may lead to an overestimation of the construction's load carrying capacity (cases 1, 2 and 12); also the consideration of the two-mode approach may sometimes be misleading and yield false conclusions (case 19).

Then, having assumed that the cross-sectional area is constant (i.e. $F = b_1 h_1 + b_2 h_2 + b_3 h_3 = \text{const}$), calculations have been carried out for the channel under discussion. Figure 13 shows the dimensionless first global stress σ_1^* $(m = 1)$ and the first local stress σ_2^* $(m = 10)$ plotted against the flange to web width ratio b_2/b_1 (where $b_3 = b_1$) on the assumption that the thickness of all walls is identical and constant $(h_1 = h_2 = h_3 = \text{const})$. Figure 14 presents dimensionless stresses σ_1^* and σ_2^* as a function of the thickness of the channel walls l/h_1 on the assumption that the flange to web the width ratio is constant $(b_2/b_1 = b_2/b_3 = 2.0)$ and that $h_1 = h_2 = h_3$. Another assumption is the constancy of the channel length. In Fig. 13 an increase in b_2/b_1 ratio causes an increase in the value of σ_1^* which results from the growing polar moment of inertia and an increase in σ_2^* stresses since flexural rigidity of channel webs becomes higher. In Fig. 14 the rising l/h_1 ratios cause an increase in σ_1^* which results, as previously, from an increase in the polar moment of inertia and a decrease in σ_2^* as flexural rigidity of channel webs lowers. In the last case the webs are the element responsible for the loss of the local stability.

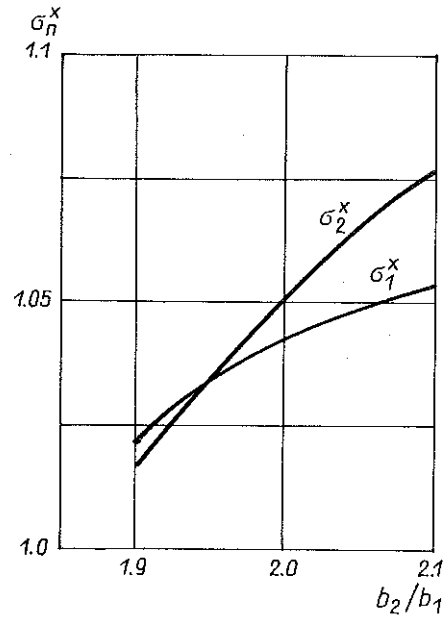

FIG.13. Relationship between dimensionless stress σ_n^* and the width b_2/b_1.

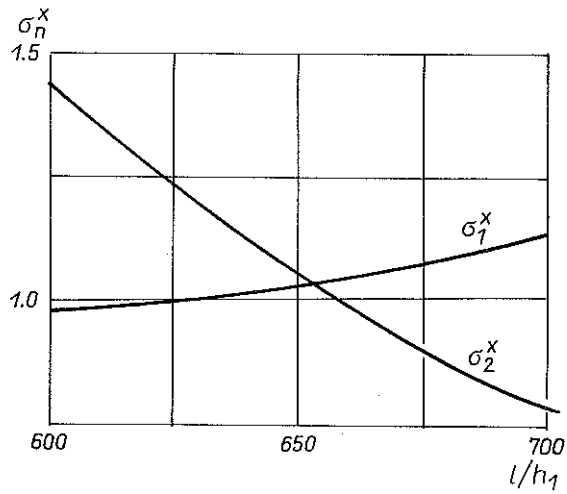

FIG. 14. Relationship between stresses σ_n^* and l/h_1.

The next figure (Fig. 15) presents the two first global and local values of nondimension stresses σ_n^* in terms of the angle $\phi_{i,i+1}$ between walls of the discussed channel:

$$b_1/b_2 = 0.5, \quad b_3/b_2 = 0.5, \quad h_1/h_2 = 1, \quad h_3/h_2 = 1,$$
$$b_2/h_2 = 50, \quad l/b_2 = 13.$$

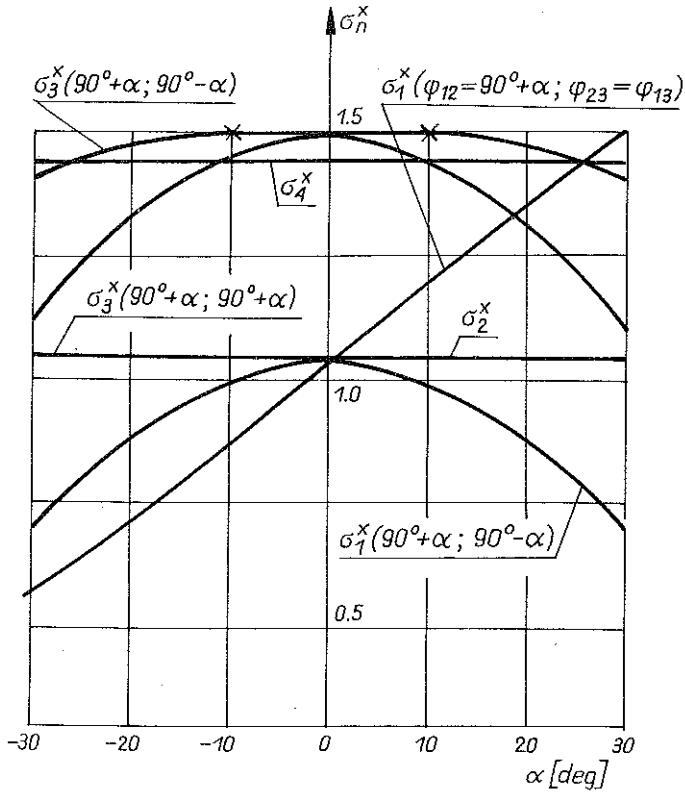

FIG. 15. Relationship between stresses σ_n^* and the auxiliary angle α.

In this figure an auxiliary angle α is introduced between walls of the channel ($\phi_{i,i+1} = 90° \pm \alpha$). If α changes, a substantial decrease is found in the value of the first overall load σ_1^* at angles $\phi_{12} = 90° + \alpha$; $\phi_{23} = 90° - \alpha$; the second global load $\sigma_3^*(m = 1)$ at angles $\phi_{12} = \phi_{23} = 90° + \alpha$; and a relatively small change in the value of σ_3^* at $\phi_{12} = 90° + \alpha$ and $\phi_{23} = 90° - \alpha$. In the latter case stress σ_3^* reaches its maximum value at $\alpha = \pm 10°$. The only exception is the first overall load σ_1^* at $\phi_{12} = \phi_{23} = 90° + \alpha$ which increases along with the increase in angle α. It is a result of different buckling modes for different α angles (see Figs. 16). At the same time values of local load $\sigma_2^*(m = 10)$ and $\sigma_4^*(m = 10)$ remain virtually constant, their changes being practically negligible, This fact can be explained in the following way. While determining approximate values of load, corresponding to the local modes under conditions of meeting, we are able to take into account only the situation where the angle is constant and bending moments are equal, moreover, the deflection function w_i for individual plates is assumed to be zero at the points of the junction.

The Byskov and Hutchinson theory, applied here, reduces all kinds of imperfections to such imperfections that correspond to initial deflections of

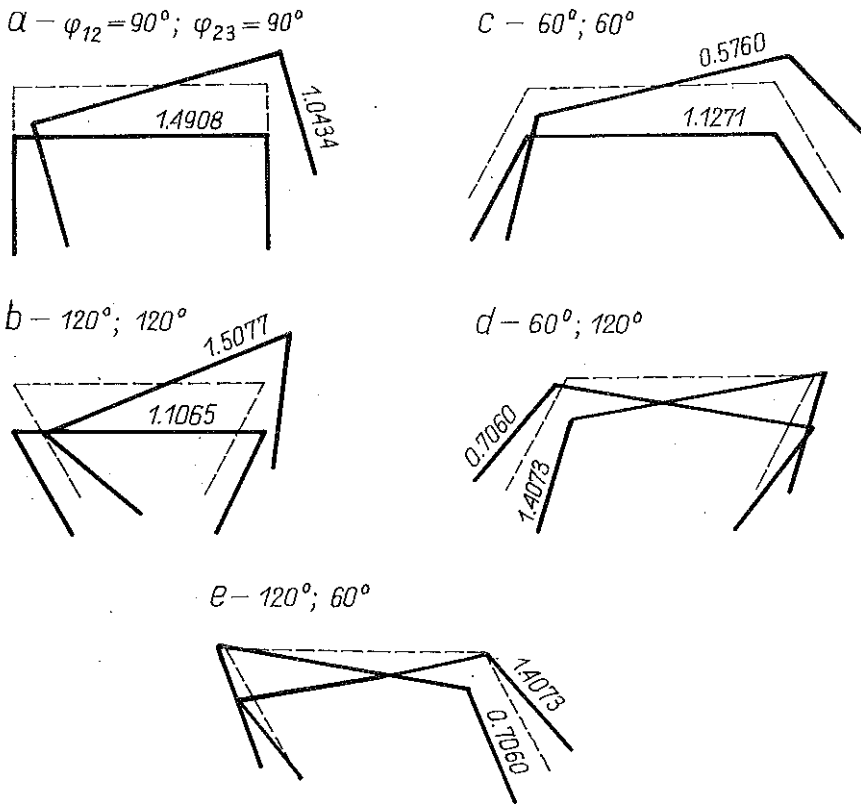

FIG. 16. Two global modes at different angles $\phi_{i,i+1}$.

a thin-walled structure: non-linear cofficients a_{ijJ} (3.8) remain constant. Not all kinds of imperfections can be reduced to a single type. Calculations of slight deviations of load and geometrical dimensions allow to obtain "proper" imperfection sensitivity of constructions as well as to find out, whether the assumed model of single type imperfection is correct (see [18] for more detailed discussion).

Figs. 16 (a to e) present the first two global buckling modes for various extreme values of angles between walls of the channel under consideration (Fig 15). In the cross-section with a vertical symmetry axis (Fig 16 a to c) two distinct global modes can be found, namely the flexural-torsional and the flexural (Euler) ones. In the two other cases (Figs. 16 d to e) this distinction is more difficult to find.

Hence the technical theory of buckling, even if used for the determination of global load values for thin-walled beams may lead to considerable discrepancies in comparison with the assumed here description of global buckling by means of nonlinear Kármán's equations.

Figure 17 presents the dimensionless stress σ_n^* as a function of the width of channel flange $b_1/b_2 = b_5/b_4$, other dimensions of column being constant (Fig. 12b)

$$b_2/b_3 = b_4/b_3 = 0.5, \quad h_1/h_3 = h_2/h_3 = h_4/h_3 = h_5/h_3 = 1.0, \quad l/b_3 = 13.$$

The plot can be divided into four parts. The significance of Interval I, $0 \leqslant b_1/b_2 \leqslant 0.025$, is merely theoretical since $b_1/h_2 \leqslant 1$ for these values. The global loads ($m = 1$) increase in this interval as a result of an increase in the height of column webs ($b_2 \cong b_2 + h_3$; $b_1 = b_5 \cong 0$). That, in turn, causes a reduction of local load values. In Interval II, $0.025 \leqslant b_1/b_2 \leqslant 0.15$, values of load increase rapidly. It is a consequence of the increased flexural rigidity of the channel flanges. In Interval III, $0.15 \leqslant b_1/b_2 \leqslant 0.5$, values of local load stabilize. The flange has on influence only an torsional not on flexural rigidity. Moreover, in the same interval a further increase in secondary global load takes place. Interval IV, $b_1/b_2 \leqslant 0.5$, is characterized by a slow monotone decrease in the values of load σ_n^*. The flange appears to be the "weakest" part of the column

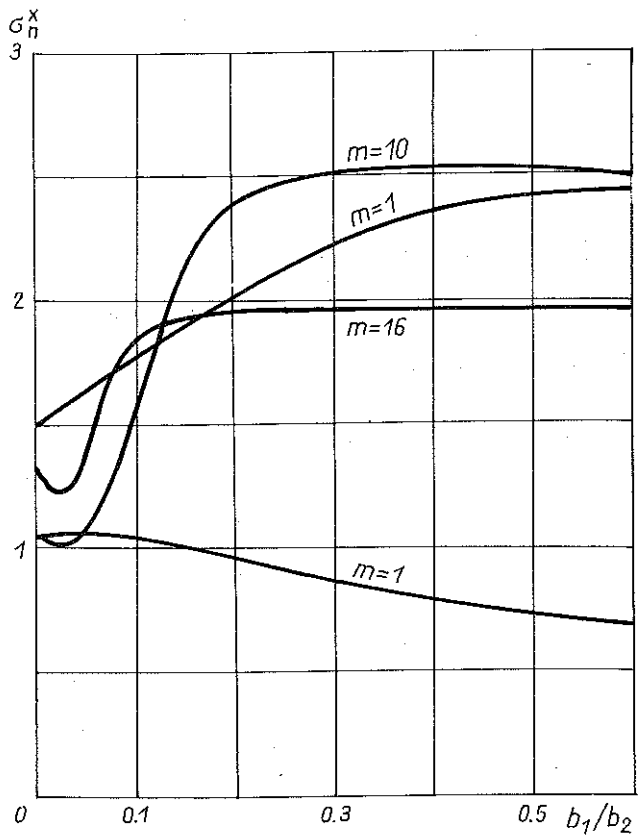

FIG. 17. The dimensionless stresses σ_n^* vs b_1/b_2.

responsible for the loss of stability. For the primary global load only a slow decrease in $\sigma^*(m = 1)$ load can be observed in Intervals II–IV.

Figure 18 shows a global mode for the considered channel, the ratio of its walls being $b_1/b_2 = b_5/b_4 = 0.5$. Also in this case two kinds of global buckling can be seen: flexural-torsional and flexural.

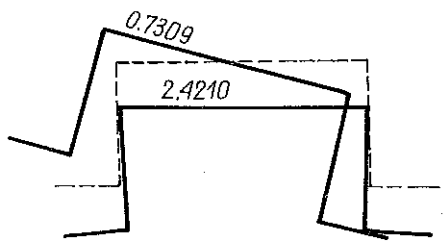

FIG. 18. Global modes for the flange width $b_1/b_2 = b_5/b_4 = 0.5$.

Table 4 contains results of calculations for an open beam, compressed eccentrically (Fig. 12c), whose geometrical dimensions are:

$$b_2/b_1 = b_3/b_1 = 3.0, \quad b_4/b_1 = 1.0, \quad l/b_1 = 20.0,$$
$$h_2/h_1 = h_3/h_1 = h_4/h_1 = 1.0, \quad b_2/h_2 = 100.0.$$

In this table the following data are presented: the eccentricity of the point of application of compressive force for a global coordinate system η, ϑ; respective values of stress distribution at characteristic points of the cross-section (ratio of stress σ_i^* at the point "i" to the maximum stress $\sigma_{\max}^*$ applied to the beam); values of global and local stresses, σ_1^* and σ_2^*, respectively; number of half-waves m corresponding to the local buckling mode; σ_1^*/σ_2^* and σ_s^*/σ_m^* ratios when only two buckling modes for imperfections $\bar{\xi}_1 = |1.0|$, $\bar{\xi}_2 = |0.2|$ are taken into consideration. Dimensions of the beam's cross-section as well as the eccentricity of the point of application of compressive force have been assumed to be analogous to those in [14] where only the critical value of the local load have been determined. It is not difficult to find out that even interactions of two buckling modes, that significantly differ from each other ($\sigma_1^*/\sigma_2^* > 3.9$), may largely diminish the load carrying capacity of the construction.

On the basis of the results obtained, one can conclude that our calculations should take into account an interaction of three buckling modes: the global and the most dangerous first and second local (having the same number of half-waves) ones (see Table 1 — case 12 and Table 2 — case 12) as well as for the influence of the value of imperfection on the number of half-waves of the local buckling. Attention should be also paid to the proper selection of local and global (the latter for open beams) buckling modes (compare Table 3 — cases 8 and 16). This can be accomplished only by means of nonlinear analysis.

Table 4. Load-carrying capacity for the open beam of following cross-section dimensions
$b_2/b_1 = 3.0$, $b_3/b_1 = 3.0$, $b_4/b_1 = 1.0$, $h_2/h_1 = 1.0$,
$h_3/h_1 = 1.0$, $h_4/h_1 = 1.0$, $b_2/h_2 = 100.0$, $l/b_1 = 20.0$,
at imperfections $\bar{\xi}_1 = |1.0|$, $\bar{\xi}_2 = |0.2|$

	Loading eccentricity		$\sigma_i^*/\sigma_{\max}^*$					σ_1^*	σ_2^*	m	σ_1^*/σ_2^*	σ_s^*/σ_m^*
	u_ξ	u_η	0	1	2	3	4					
1	0.0	0.0	1.0	1.0	1.0	1.0	1.0	1.8161	0.3743	6	4.85	0.9445
2	40.0	0.0	0.198	0.5	−0.115	0.794	1.0	3.2383	0.6988	7	4.63	0.7938
3	40.0	40.0	−0.189	−0.054	0.596	1.0	0.784	2.6032	0.5190	7	5.02	0.9435
4	40.0	−40.0	0.369	0.722	−0.455	0.606	1.0	3.9090	0.7911	8	4.94	0.7707
5	0.0	40.0	0.026	−0.205	1.0	0.305	−0.097	5.0459	0.6861	7	7.35	0.9001
6	−40.0	40.0	0.133	−0.241	1.0	−0.122	−0.536	8.4789	0.9111	8	9.31	0.9525
7	−40.0	0.0	0.619	0.251	1.0	−0.106	−0.356	4.2532	0.6654	7	6.39	0.9471
8	−40.0	−40.0	1.0	0.882	0.343	−0.012	0.168	2.6635	0.5834	7	4.57	0.8420
9	0.0	−40.0	0.772	1.0	−0.204	0.483	0.885	2.8522	0.7294	7	3.91	0.8101

The calculations carried out and, indirectly, the results published in [8, 16] make use state, with the precision sufficient for engineering purposes, that taking into account only the first order approximation of the interaction of three buckling modes can serve as a lower estimation of load carrying capacity. Such an estimation enables to avoid serious numerical problems occuring when the second order solution is considered for typical thin-walled structures.

5. Conclusions

The initial postbuckling behaviour of thin-walled closed and open beams under nonuniform compression by means of the transition matrix method has been presented. The present approach regards the secondary local mode activated by the interaction of an overall mode with the primary local mode. Rational dimensions of the beams can be determined on the assumption of the plate model. The imperfection-sensitivity can be lowered provided that the beam parameters are selected entirely by means of the nonlinear analysis. The assumption of a single type of imperfection is quite questionable. In the case when critical stresses of a few buckling modes are comparable the disregarding of the mode interaction may lead to overestimating the load carrying capacity of the structure.

The present analysis has to be completed by including the second order solution in order to investigate postbuckling in cases when the first order of the interaction is weak.

References

1. E. Byskov and J. W. Hutchinson, *Mode interaction in axially stiffened cylindrical shells*, AIAA J., **15**, 7, pp 941–948, 1977.
2. W. T. Koiter and A. van der Neut, *Interaction between local and overall buckling of stiffened compression panels, Part I, II, Thin-walled structures* (Edited by J. Rhodes and A. C. Walker), Granada, London, pp. 61–85, 1980.
3. S. Sridharan and M. A. Ali, *An improved interactive buckling analysis of thin-walled having doubly symmetric sections*, Int J. Solids Struct., **22**, 4, pp. 429–443, 1986.
4. H. Møllmann and P. Goltermann, *Interactive buckling in thin-walled beams, Part. I. Theory*, The Danish Center for Applied Mathematics and Mechanics, The Technical University of Denmark, Report No. 344, 1987.
5. P. Goltermann and H. Møllmann, *Interactive buckling in thin-walled beams*, Part 2: Applications, The Danish Center for Applied Mathematics and Mechanics, The Technical University of Denmark, Report No. 345, 1987.
6. M. Pignataro and A. Luongo, *Asymmetric interactive buckling of thin-walled columns with initial imperfections*, Thin-walled Structures, **5**, 5, pp. 365–386, 1987.
7. Z. Kołakowski *Some thoughts of mode interaction in thin-walled column uniform compression* Thin-Walled Structures **7**, 23–35, 1989.

8. E. BYSKOV, *Elastic buckling problem with infinitely many local modes*, The Danish Center for Applied Mathematics and Mechanics, The Technical University of Denmark, Report No. 327, 1986.
9. R. BENITO and S. SRIDHARAN, *Mode interaction in thin-walled structural members*, J. Struct. Mech, **12**, 4, pp. 517–542, 1984–85.
10. D. Hui, *Design of beneficial geometric imperfections for elastic collapse of thin-walled box columns*, Int. J. Mech. Sci, **28**, 3, pp. 163–172, 1986
11. E. BYSKOV, *An asymptotic expansion applied to van der Nuet's column, Collapse: The buckling of structures in theory and practise* (Edited by J. M. T. THOMPSON and G. W. HUNT), Cambridge University Press, Cambridge, pp. 269–282, 1983.
12. Z. KOŁAKOWSKI, *Mode intraction in thin-walled trapezoidal column under uniform compression*, Thin-walled Structures, **5**, 5, pp. 329–342, 1987.
13. B. UNGER, *Elastisches Kippen von beliebig gelagerten und aufgehängten Durchlaufträgern mit einfachsymmetrischen, in Trägerachse veränderlichem Querschnitt und einer Abwandlung des Reduktionsverfahrens als Lösungsmethode*, Dissertation D17, Darmstadt 1969.
14. K. KLÖPPEL and W. BILSTEIN, *Ein Verfahren zur Ermittlung der Beullasten beliebiger rechtwinkling abgekanteter offener und geschlossener Profile nach der linearen Beultheorie unter Verwendung eines abgewandelten Reduktionsverfahrens*, Veröffentlichungen des Institutes für Statik und Stahlbau der Technischen Hochschule Darmstadt, Heft 16, 1971.
15. W. BILSTEIN, *Beitrag zur Berechnung vorverformter mit diskreten Längssteifen ausgesteifter, ausschliesslich in Längsrichtung belasteter Rechteckplatten nach der nichtlinearen Beultheorie*, Der Stahlbau, Heft 7, pp. 193–201, and Heft 9, pp. 276–282, 1974.
16. А. МАНЕВИЧ, *К теории связанной потери устойчивости подкрепленных тонкостенных конструкций*, Прикл. Математ. и Мех., **46**, 2, 337–345, 1982.
17. Z. KOŁAKOWSKI *Some aspects of mode interaction in thin-walled stiffened plate under uniform compression*, Engineering Transactions, **36**, 1, 167–179, 1988.
18. Z. KOŁAKOWSKI, *Mode interaction in wide plate with angle section longitudinal stiffeners under compression*, Engineering Transactions, **37**, 1, 117–135, 1989.

STRESZCZENIE

WSPÓŁDZIAŁANIE RÓŻNYCH POSTACI WYBOCZENIA BELEK O PRZEKROJACH CIENKOŚCIENNYCH OTWARTYCH I ZAMKNIĘTYCH

Rozważano wpływ wzajemnego oddziaływania bliskich sobie postaci wyboczenia dzwigarów cienkościennych na ich zachowanie się po wyboczeniu. Zajęto się przypadkiem działania osiowego ściskania i stałego momentu zginającego na belki o otwartych i zamkniętych przekrojach cienkościennych, swobodnie podparte na obu końcach. Zastosowano rozwinięcia asymptotyczne BYSKOVA i HUTCHINSONA [1] w obliczeniach numerycznych związanych z metodą macierzy przejścia. Celem pracy jest przeprowadzenie ściślejszej analizy przebiegu procesu następującego bezpośrednio po wyboczeniu w konstrukcjach z imperfekcjami, z uwzględnieniem wpływu współdziałania kilku bliskich sobie postaci wyboczenia. Obliczenia przeprowadzono dla różnych typów belek.

Резюме

ВЗАИМОДЕЙСТВИЕ РАЗНЫХ ВИДОВ БОКОВОГО ВЫПУЧИВАНИЯ БАЛОК С ТОНКОСТЕННЫМИ ОКТРЫТЫМИ И ЗАМКНУТЫМИ СЕЧЕНИЯМИ

Обсужалось влияние взаимодействия подобных по виду боковых выпучиваний тонкостенных несущих болок на их поведение после потери устойчивости. Был рассмотрен случай воздействия осевого сжатия и изгибного момента на балки с открытыми и замкнутыми тонкостеными сечениями, свободно опертыми на обоих концах. Использовалось асимптотическое разложение Быскова и Хачинсона [1] в численных расчетах, связанных с методом матриц перехода. Цель работы заключалась в проведении точностного анализа процесса, наступающего после выпучивания в конструкциях с имерфекциями, с учетом влияния взаимодействия нескольких подобнъх по виду боковых выпучиваний. Расчеты были проведены для балок разных типов.

INSTITUTE OF APPLIED MECHANICS
TECHNICAL UNIVERSITY OF ŁÓDŹ.

Received December 2, 1988.